The 2012 World Congress on
Advances in Civil, Environmental, and Materials Research (ACEM' 12)
Seoul, Korea, August 26-30, 2012

Flutter and Gust Response Analysis of the Messina Strait Bridge

– Benchmark Study –

*Hiroshi Tanaka[1)] Akihide Hatanaka[2)] Saang-Bum Kim[3)] and Jong-Ho Yang[4)]

[1)3) 4)] *Engineering & Construction Group of*

SAMSUNG C&T CORPORATION, Seoul 137-956, Korea

tnk.h@samsung.com

Technology HQ. of NICHIZO TECH INC., Osaka 551-0023, Japan

ABSTRACT

Samsung C&T did flutter and gust response analysis and compared these results with those of Politecnico di Milano (PDM) and Yokohama National University as the benchmark study of Messina Strait Bridge.

Main results here are as followings;

●Flutter wind velocity is over 80 m/s and its frequency and logarithmic damping agree well to the experimental results of PDM.

●The flutter mode shape is consisting of multi-modes and asymmetrical.

●Results of the gust analysis agree well to those of experimental results of PDM by applying our modification of Davenport's coherence formula and the use of measured admittances for lift and moment forces.

1. INTRODUCTION

One of the most important key technologies for the construction of the Messina Strait Bridge (i.e. the Messina Bridge for abbreviation) is the assessment of aerodynamic stability. Diana (2001) of PDM Group proposed the benchmark study on the Messina Bridge during 10th ICWE in 1999. Miyata (2003) of Yokohama National University (YNU) firstly replied the proposal presenting flutter analysis by using many models with different methods. Their results of the research were summarized as followings:

- As a structural model, AM1 model gives the closest frequencies and modal shapes to those of PDM by eigenvalue analysis.
- Flutter critical wind speeds of YNU are all lower than that of PDM.
- Flutter mode shape of AM1 and BM2 models are anti-symmetric and agrees with mode shape of PDM.
- Wind induced static deflections (i.e. horizontal and torsion) of decks show good agreement with those of PDM.

On the other hand, Samsung C&T (i.e. Samsung for abbreviation) has been developing the new technologies on aerodynamics for super long span suspended bridges. Our main research target are as follows;

[1), 4)] Bridge Engineer
[2), 3)] Aerodynamics Researcher

●Development of flutter analysis
●Development of gust response analysis (Power Spectrum & Time domain methods)
●Benchmark study to improve our software

SAMSUNG did flutter and gust response analysis and compared these results with those of PDM and YNU as a benchmark study of Messina Strait Bridge.

The purpose of the benchmarking is to contribute the wind engineering and to improve our software.

2. ANALYTICAL BACK GROUND

2.1 Structural Model and Dimension

The Messina Bridge will connect Sicily with Southern mainland Italy (Fig. 1). However the construction of the bridge has been interrupted by the political reason now. This gives us the chance to do the benchmarking. After completion, the Messina Bridge will surplus the Akashi Kaikyo Bridge in scales (Table 1).

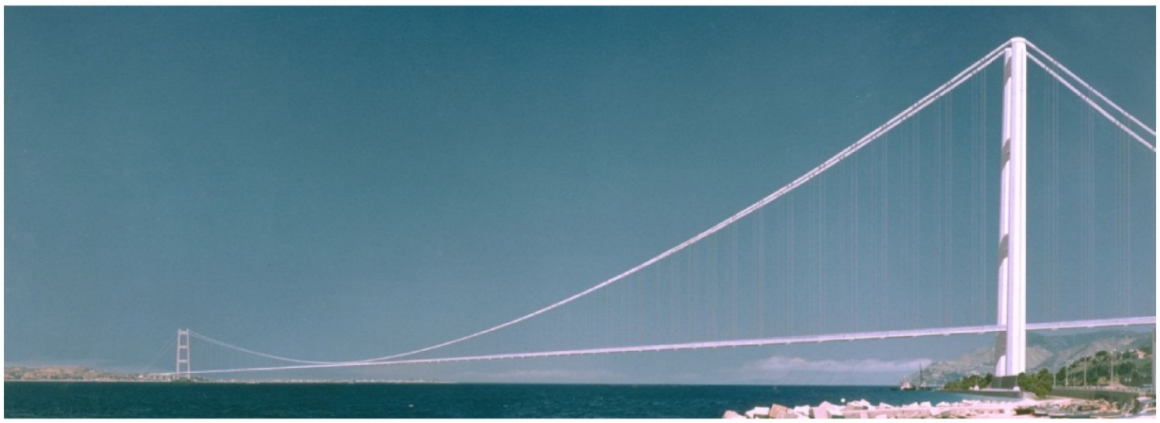

Fig. 1. The Messina Straits Bridge (Stretto di Messina S.p.A 2009)

Table 1. Dimensions of the Messina Bridge comparing with the Akashi Kaikyo Bridge

Longest span	3300m (Akashi-Kaikyo 1991m)
Tower height	382.6m (298.3m)
Deck width	60.4m (35.5m)
Cable diameter	4 x 1.24m (2 x 1.12m)
Design wind speed	75m/s (80m/s)

FEM model is applied by using beam model for static and dynamic (i.e. flutter and gust response) analysis. When we tried to transfer the PDM`s input data to our in-house software, we met difficulty in handling data format. YNU kindly supplied their data to us. Therefore our model is identical to the AM1 model of YNU as shown in Fig. 2. AM1 model is almost equivalent to that of PDM (Miyata 2003).

.

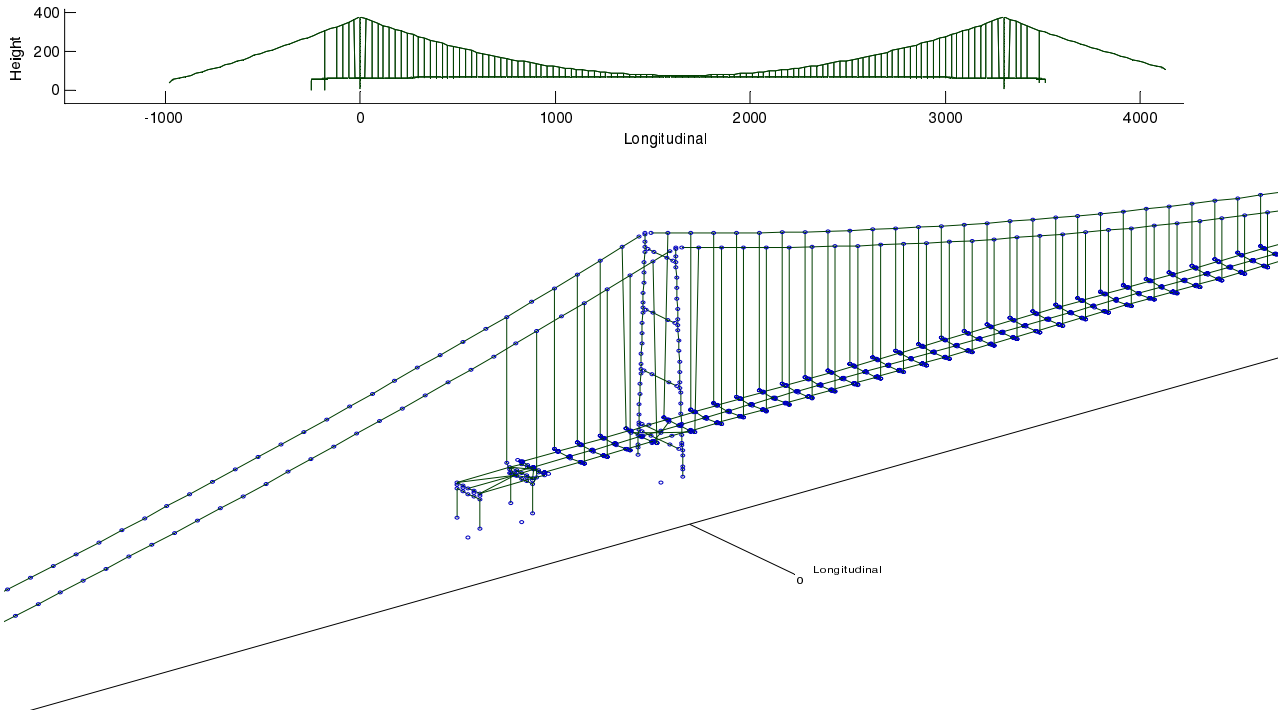

Fig. 2 FEM Model of the Messina Bridge

2.2 Deck Section and Dimension (Stretto di Messina S. p. A 2009)

The suspended deck section consists of three stream-lined longitudinal boxes; the lateral ones for the two road carriageways and the center one for railways as shown in Fig 3. The height of the deck is 4.68m (i.e. cross sectional area: A=4.68m^2/m). Full width of the deck is 60.4m however 60m is applied as a cross sectional width: B for flutter analysis (i.e. B = 60m). Deck and cable weight are 18.1 and 37 t/m respectively.

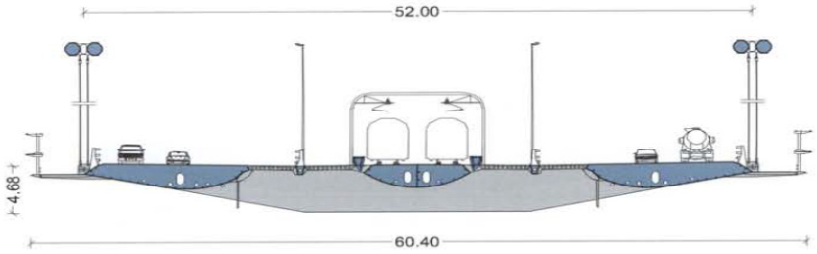

Fig. 3 Cross Section of Deck (Stretto di Messina S.p.A 2009)

2.3 Static Aerodynamic Force Coefficients

The definition of static aerodynamic force coefficients for our computer program is as

Eq. (1) based upon Japanese code (HSB 2002). The given drag coefficient (C_D) data of PDM were converted by the use of A (cross section area per unit length [m^2/m]) instead of B (cross sectional width [m]).

$$P_i = \frac{1}{2}\rho V^2 C_D A \qquad L_i = \frac{1}{2}\rho V^2 C_L B \qquad M_i = \frac{1}{2}\rho V^2 C_M B^2 \tag{1}$$

where P_i, L_i and M_i are respectively drag, lift, and moment aerodynamic force per unit length (Fig. 4). ρ is the air density [$t \cdot s^2/m^4$], V is the mean wind velocity [m/s], v (t) and w(t) are the fluctuating wind velocity [m/s] (See chapter 4). Table 2 shows the digital data at α = 0 deg. C_D , C_L and C_M are drag, lift and moment coefficient respectively(Fig. 5).

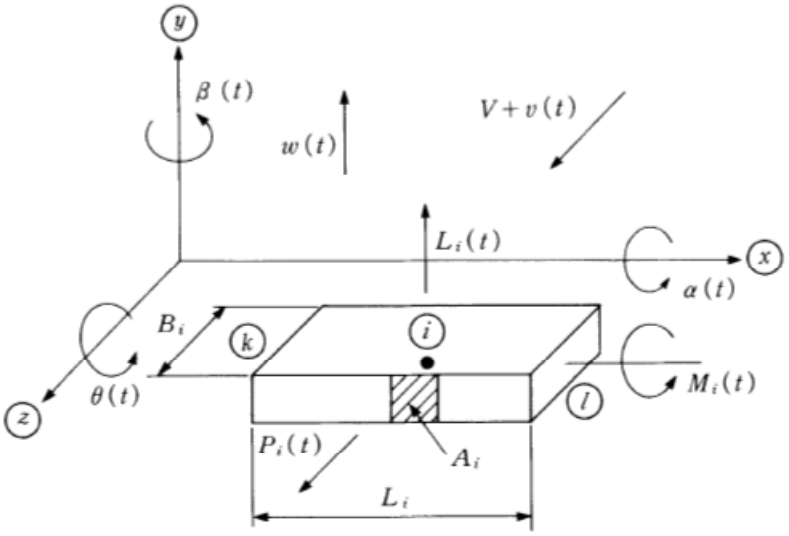

Fig. 4 Definition of P_i, L_i and M_i and Member (i) in Global Coordinate

Table 2 Static Aerodynamic Force Coefficients (at α = 0 deg.)

C_D	1.164
$dC_D/d\alpha$	2.086
C_L	-0.053
$dC_L/d\alpha$	0.765
C_M	0.020
$dC_M/d\alpha$	0.198

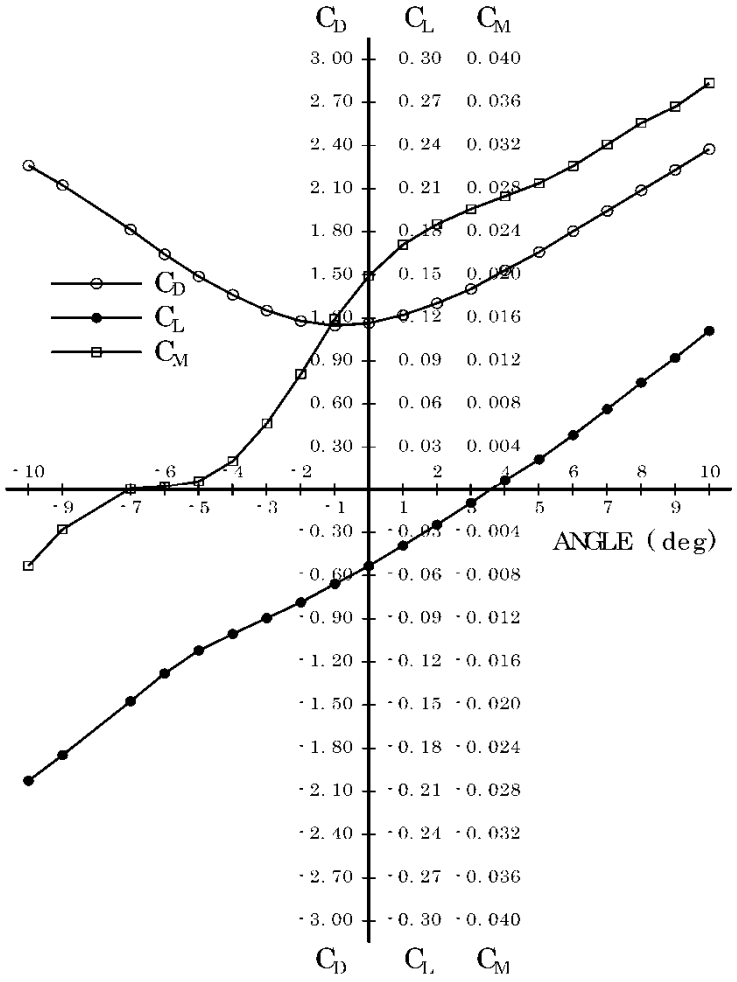

Fig. 5 Static Aerodynamic Force Coefficients

2.4 Flutter Derivatives

Through inter-net, PDM has been supplying such flutter derivatives as H_i^* and A_i^* *(i = 1~4)* shown in Figs.6 and 7. The definition of the flutter derivative is identical to old Scanlan's convention (Scanlan R.H 1996) with the reduced frequency defined as *U/fB* where f is frequency [*Hz*] and U is wind velocity [*m/s*].

The third degree polynomial fitting curves (Figs.6 and 7) was used for the input data to flutter analysis.

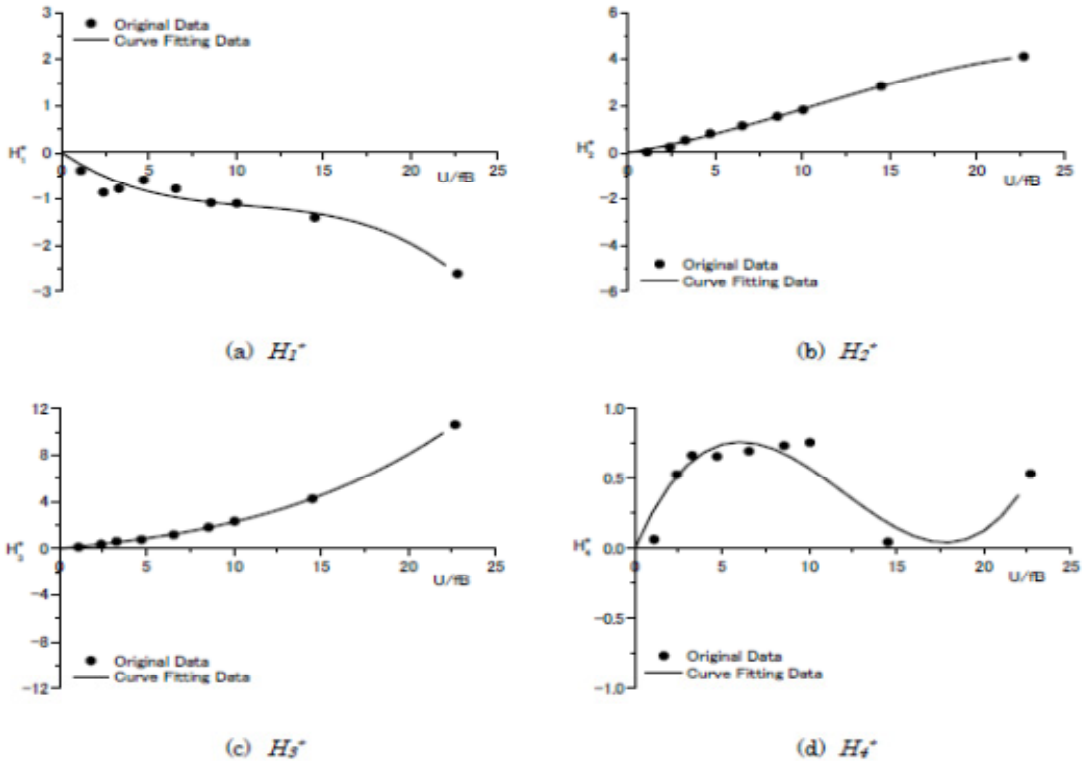

Fig.6 Flutter Derivatives H_i^* (α=0 deg.)

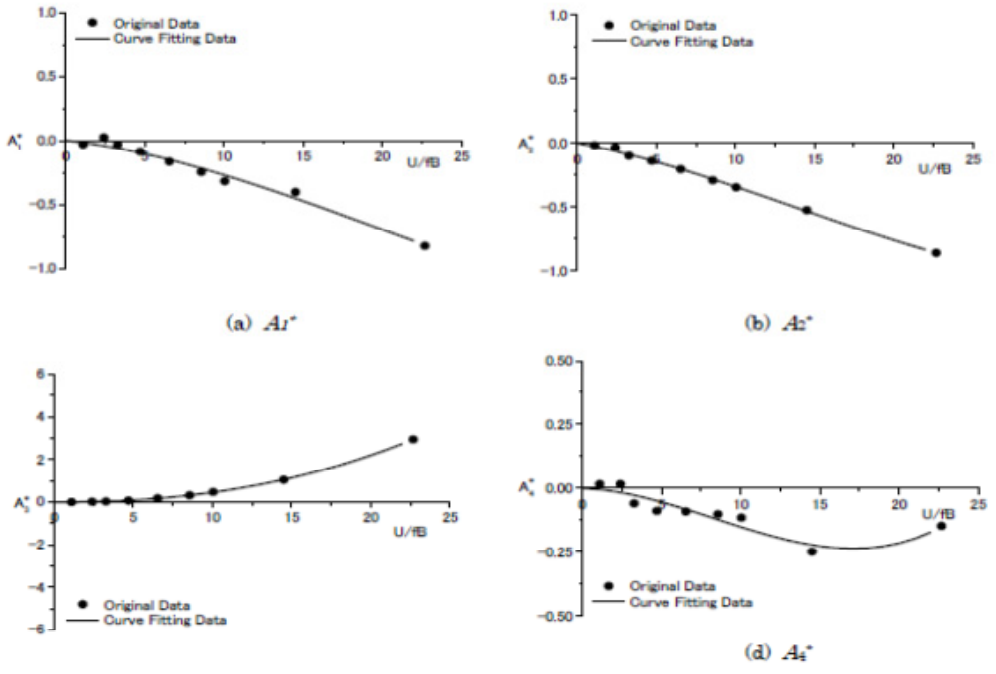

Fig.7 Flutter Derivatives A_i^* (α=0 deg.)

2.5 Eigen Mode Analysis

Main national frequencies of SAMSUNG, YNU(Yamada 2003) and PDM (Diana 1999) are compared in Table 3 and mode shapes by SAMSUNG are shown in Fig.8.

Table 3 Major National Frequencies among SAMSUNG, YNU and PDM

Mode No. of SAMSUNG	Natural Frequency (Hz)			SAMSUNG/ PDM	Mode Shape
	SAMSUNG	YNU	PDM		
1	0.031	0.031	0.033	0.94	Symmetric/lateral
2	0.059	0.059	0.059	1.00	Asymmetric/lateral
3	0.063	0.064	0.061	1.03	Asymmetric/vertical
4	0.078	0.078	0.080	0.98	Symmetric/vertical
5	0.084	0.084	0.084	1.00	Symmetric/lateral
6	0.090	0.076	0.081	1.12	Asymmetric/torsional
10	0.101	0.093	0.097	1.04	Symmetric/torsional

Mode - 1

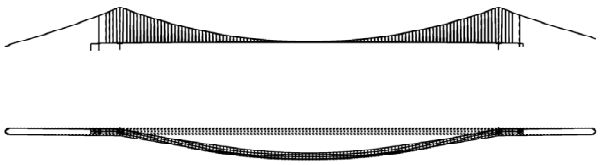

Mode - 2

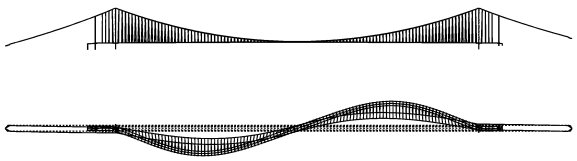

Mode – 3

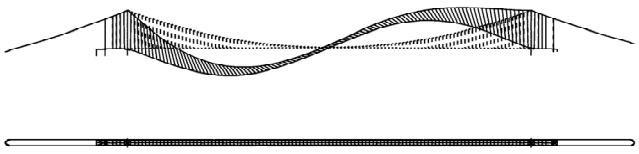

Mode – 4

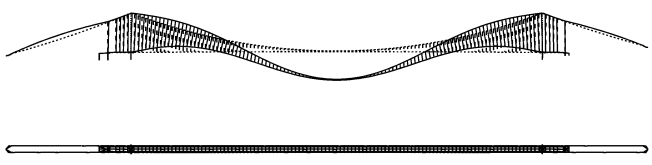

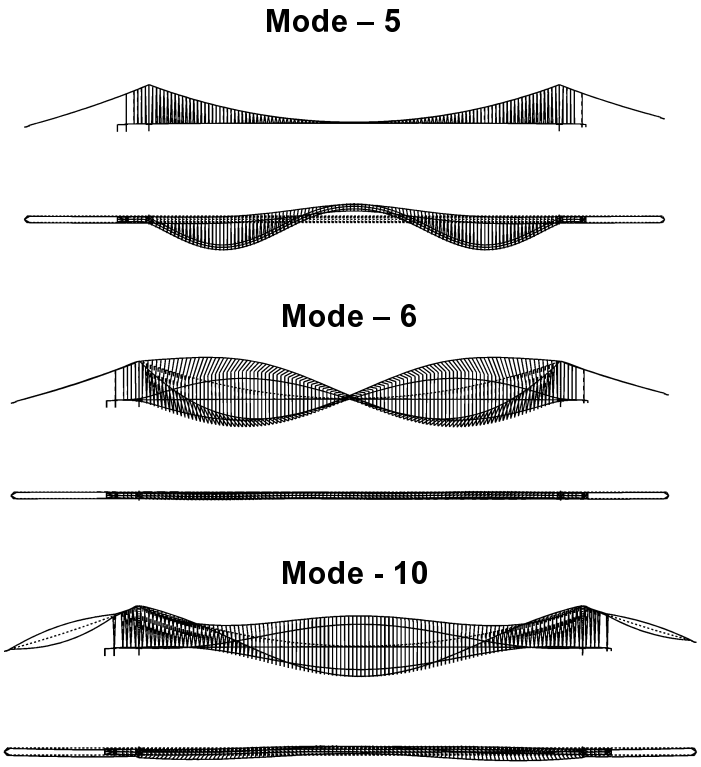

Fig. 8 Main Mode Shapes by Samsung C&T

3. FLUTTER ANALYSIS

Multi-mode flutter analysis was applied to the 3-dimensional frame model of the Messina Bridge. Tanaka and Yamamura (1993) developed the program by using flutter derivatives in matrix form. It was used to clarify the characteristics of multi-mode flutter which was observed in the wind tunnel tests of the Akashi Kaikyo Bridge. This program is based upon Scanlan (1978). We revised Tanaka (1993) by increasing flutter derivatives as we will express in this chapter.

3.1 Dynamic Equation

Extension of Scanlan's formulation leads to dynamic equations in matrix form by the displacement method. First, the equations of motion of girders are expressed as (see Fig.1 for notation),

$$[M] \cdot \{\ddot{U}_i(t)\} + [C] \cdot \{\dot{U}_i(t)\} + [K] \cdot \{U_i(t)\} = \{F_i(t)\} \qquad (2)$$

where [*M*] is the mass matrix, [*C*] is the structural damping matrix, [*K*] is the stiffness matrix, $\{U_i(t)\} = \{x_i(t),\ y_i(t),\ z_i(t),\ \alpha_i(t),\ \beta_i(t),\ \theta_i(t)\}$ is the displacement vector of a member *(i)*, and $\{F_i(t)\}$ is the wind load vector(=self-excited force). The displacement vector, $\{U_i(t)\}$ is expressed by eigen-mode functions $\{\emptyset_i(t)\}$ and generalized coordinates $X_m(t)$, where m=1, 2,… M. M is the number of modes, as follows:

$$\left.\begin{aligned} &\{U_i(t)\} = \sum_{m=1}^{M} \{\phi_{im}\} \cdot X_m(t) \\ &\emptyset_{im} = (\emptyset_{km} + \emptyset_{lm})/2 \ \text{(Mode shape at the center of } i\text{ - th member)} \end{aligned}\right\} \quad (3)$$

Pre-multiplying Eq. (2) by $\{\emptyset_{im}\}^T$, it becomes

$$\left.\begin{aligned} &\ddot{X}_m(t) + 2h_m^s \cdot \omega_m \cdot \dot{X}_m(t) + \omega_{\mathrm{m}}^2 \cdot Xm(t) = \{\emptyset_{im}\}^T \cdot F_i(t)/M_m^* \\ &M_m^* = \{\emptyset_{im}\}^T \cdot [M] \cdot \{\emptyset_{im}\} \end{aligned}\right\} \quad (4)$$

where h_m^s and ω_m are, respectively, the structural damping ratio in still air and circular frequency [*rad/s*] of the *m*-th mode. Under the assumption that the girder is regarded as horizontal and the wind acts on bridge laterally at right angle, the components of wind vector $\{F_i(t)\}$ in Eq.(4) can be expressed as

$$\{F_i(t)\} = \{0,\ L_i(t),\ P_i(t), M_i(t), 0, 0\} \quad (5)$$

$$\left.\begin{aligned} P_i(t) &= (\rho \cdot V_i^2/2) \cdot A_i \cdot K_i \cdot [P_{0i}^*, P_{1i}^*,\ P_{2i}^*,\ P_{3i}^*,\ P_{4i}^*, P_{5i}^*] \\ &\quad \cdot \{\dot{y}_i(t)/V_i, \dot{z}_i(t)/V_i, B_i \cdot \dot{\alpha}_i(t)/V_i, K_i \cdot \alpha_i(t), K_i \cdot y_i(t)/B_i, K_i \cdot z_i(t)/B_i\} \cdot L_i \\ L_i(t) &= (\rho \cdot V_i^2/2) \cdot B_i \cdot K_i \cdot [H_{0i}^*,\ H_{1i}^*,\ H_{2i}^*,\ H_{3i}^*,\ H_{4i}^*,\ H_{5i}^*] \\ &\quad \cdot \{\dot{z}_i(t)/V_i, \dot{y}_i(t)/V_i, B_i \cdot \dot{\alpha}_i(t)/V_i, K_i \cdot \alpha_i(t), K_i \cdot y_i(t)/B_i, K_i \cdot z_i(t)/B_i\} \cdot L_i \\ M_i(t) &= (\rho \cdot V_i^2/2) \cdot \mathrm{B}_\mathrm{i}^2 \cdot K_i \cdot [A_{0i}^*,\ A_{1i}^*,\ A_{2i}^*,\ A_{3i}^*,\ A_{4i}^*,\ A_{5i}^*] \\ &\quad \cdot \{\dot{z}_i(t)/V_i, \dot{y}_i(t)/V_i, B_i \cdot \dot{\alpha}_i(t)/V_i, K_i \cdot \alpha_i(t), K_i \cdot y_i(t)/B_i, K_i \cdot z_i(t)/B_i\} \cdot L_i \end{aligned}\right\} \quad (6)$$

$K_i = B_i \cdot \omega/V_i \fallingdotseq B_i \cdot \omega_R/V_i$: the reduced flutter frequency [see Eq.(17)]

$$\left.\begin{aligned} &P_{0i}^* = -(dC_D/d\alpha)/K_i = -\mathrm{C}'_{\mathrm{Di}}/K_i, \quad P_{1i}^* = -2C_{Di}/K_i, \quad P_{2i}^* \fallingdotseq 0 \\ &P_{3i}^* = (dC_{Di}/d\alpha)/K_i^2 = \mathrm{C}'_{\mathrm{Di}}/K_i^2, \qquad P_{4i}^* = 0 \\ &P_{5i}^*(K_i) = H_{5i}^*(K_i) = A_{5i}^*(K_i) = 0 \\ &H_{0i}^* = -2C_{Li}/K_i, \quad A_{0i}^* = -2C_{Mi}/K_i \end{aligned}\right\} \quad (7)$$

where $P_i(t)$, $L_i(t)$, $M_i(t)$ are, respectively, the drag force, lift force and moment. ρ is the air density [$t \cdot s^2/m^4$], V_i is the wind velocity [*m/s*], A_i is the area(per unit span) subjected to wind [m^2/m], B_i is the lateral girder width[*m*], L_i is the member length[*m*], C_{Di} is the drag coefficient defined for A_i, ω is the flutter circular frequency [*rad/s*], $P_{ji}^*(K_i) \cdot H_{ji}^*(K_i) \cdot A_{ji}^*(K_i)$ are dimensionless flutter derivatives of *i*-th member. All derivatives are double of those given by Scanlan (1978) and $H_{2i}^*(K_i) \cdot H_{3i}^*(K_i) \cdot A_{1i}^*(K_i)$ have opposite sign due to upward y-axis adopted here.

Note that the flutter derivatives of Eq.(7) are used in this paper. The eigen-mode function $\{\emptyset_{im}\}$ is defined as follows:

$$\{\emptyset_{im}\} = \left\{\emptyset_{im}^x, \emptyset_{im}^y,\ \emptyset_{im}^z,\ \emptyset_{im}^\alpha,\ \emptyset_{im}^\beta,\ \emptyset_{im}^\theta\right\} \quad (8)$$

The self-excitation terms for girders are derived by inserting Eqs.(3),(5),(6) and (8) into Eq.(4):

$$\{\emptyset_{im}\}^T \cdot \{F_i(t)\}/M_m^* = \left[\{\emptyset_{im}^z\}^T \cdot \{P_i(t)\} + \{\emptyset_{im}^y\}^T \cdot \{L_i(t)\} + \{\emptyset_{im}^\alpha\}^T \cdot \{M_i(t)\}\right]/M_m^* \qquad (9)$$

$$\left.\begin{aligned} \{\phi_{im}^z\}^T \cdot \{P_i(t)\} &= (\rho/2)\cdot\omega\cdot\sum_i A_i \cdot B_i \cdot \phi_{im}^z [P_{0i}^*, P_{1i}^*, P_{2i}^*, P_{3i}^*, P_{4i}^*, P_{5i}^*] \\ &\{\sum_n \dot{X}_n(t)\cdot\phi_{in}^y, \sum_n \dot{X}_n(t)\cdot\phi_{in}^z, B_i\cdot\sum_n \dot{X}_n(t)\cdot\phi_{in}^\alpha, B_i\cdot\omega\cdot\sum_n X_n(t)\cdot\phi_{in}^\alpha, \\ &\omega\cdot\sum_n X_n(t)\cdot\phi_{in}^y, \omega\cdot\sum_n X_n(t)\cdot\phi_{in}^z\}\cdot L_i \end{aligned}\right\} \qquad (10)$$

$$\left.\begin{aligned} \{\phi_{im}^y\}^T \cdot \{L_i(t)\} &= (\rho/2)\cdot\omega\cdot\sum_i B_i^2 \cdot \phi_{im}^y [H_{0i}^*, H_{1i}^*, H_{2i}^*, H_{3i}^*, H_{4i}^*, H_{5i}^*] \\ &\{\sum_n \dot{X}_n(t)\cdot\phi_{in}^z, \sum_n \dot{X}_n(t)\cdot\phi_{in}^y, B_i\cdot\sum_n \dot{X}_n(t)\cdot\phi_{in}^\alpha, B_i\cdot\omega\cdot\sum_n X_n(t)\cdot\phi_{in}^\alpha, \\ &\omega\cdot\sum_n X_n(t)\cdot\phi_{in}^y, \omega\cdot\sum_n X_n(t)\cdot\phi_{in}^z\}\cdot L_i \end{aligned}\right\} \qquad (11)$$

$$\left.\begin{aligned} \{\phi_{im}^\alpha\}^T \cdot \{M_i(t)\} &= (\rho/2)\cdot\omega\cdot\sum_i B_i^3 \cdot \phi_{im}^\alpha [A_{0i}^*, A_{1i}^*, A_{2i}^*, A_{3i}^*, A_{4i}^*, A_{5i}^*] \\ &\{\sum_n \dot{X}_n(t)\cdot\phi_{in}^z, \sum_n \dot{X}_n(t)\cdot\phi_{in}^y, B_i\cdot\sum_n \dot{X}_n(t)\cdot\phi_{in}^\alpha, B_i\cdot\omega\cdot\sum_n X_n(t)\cdot\phi_{in}^\alpha, \\ &\omega\cdot\sum_n X_n(t)\cdot\phi_{in}^y, \omega\cdot\sum_n X_n(t)\cdot\phi_{in}^z\}\cdot L_i \end{aligned}\right\} \qquad (12)$$

For main cables of suspension bridges, only the $P_{1i}^*(K_i)$ and $H_{1i}^*(K_i)$ terms in Eqs.(10)-(12) are necessary , and for $H_{1i}^*(K_i)$ the quasi-steady formula may be applied, yielding:

$$H_{1i}^*(K_i) = -C_{Di}/K_i = -(1/2\pi)\cdot C_{Di}\cdot V_i/(f\cdot B_i) \qquad (13)$$

where *f* is the flutter frequency [*Hz*] and B_i is the diameter of the cable [*m*]. For the tower members, only the P_{1i}^* term in Eqs.(10)-(12) are necessary and L_i in Eqs. (10)-(12) should refer to the vertical length of the members. The hanger member area subjected to the wind pressure should be included in the main cable and the girder area, weighted by the ratio of the drag coefficient of hanger to main cable or girder, respectively.

Then, a set of coupled flutter equation is obtained by inserting Eqs. (10)-(12) into Eq.(4).

$$\left.\begin{aligned} &\ddot{X}_m(t) + 2h_m^s\cdot(\omega_m/\omega)\cdot\omega\cdot\dot{X}_m(t) + \omega_m^2\cdot X_m(t) \\ &\quad = \sum_n E_{mn}\cdot\omega\cdot\dot{X}_n(t) + \sum_n F_{mn}\cdot\omega^2\cdot X_n(t) \end{aligned}\right\} \qquad (14)$$

$$\left.\begin{aligned} E_{mn} &= (\rho/2M_m^*)\cdot\sum_i B_i\cdot\{\phi_{im}^y, \phi_{im}^z, \phi_{im}^\alpha\}^T\cdot[H]\cdot\{\phi_{im}^y, \phi_{im}^z, \phi_{im}^\alpha\}\cdot L_i \\ [H] &= \begin{bmatrix} H_{1i}^*(K_i)\cdot B_i & H_{0i}^*(K_i)\cdot B_i & H_{2i}^*(K_i)\cdot B_i^2 \\ P_{0i}^*(K_i)\cdot A_i & P_{1i}^*(K_i)\cdot A_i & P_{2i}^*(K_i)\cdot A_i\cdot B_i \\ A_{1i}^*(K_i)\cdot B_i^2 & A_{0i}^*(K_i)\cdot B_i^2 & A_{2i}^*(K_i)\cdot B_i^3 \end{bmatrix} \end{aligned}\right\} \qquad (15)$$

$$F_{mn} = (\rho / 2M_m^*) \cdot \sum_i B_i \cdot \{\phi_{im}^y, \phi_{im}^z, \phi_{im}^\alpha\}^T \cdot [\Omega] \cdot \{\phi_{im}^y, \phi_{im}^z, \phi_{im}^\alpha\} \cdot L_i$$

$$[\Omega] = \begin{bmatrix} H_{4i}^*(K_i) \cdot B_i & H_{5i}^*(K_i) \cdot B_i & H_{3i}^*(K_i) \cdot B_i^2 \\ P_{4i}^*(K_i) \cdot A_i & P_{5i}^*(K_i) \cdot A_i & P_{3i}^*(K_i) \cdot A_i \cdot B_i \\ A_{4i}^*(K_i) \cdot B_i^2 & A_{5i}^*(K_i) \cdot B_i^2 & A_{3i}^*(K_i) \cdot B_i^3 \end{bmatrix} \quad (16)$$

3.2 COMPLEX EIGENVALUE EQUATIONS

The complex generalized coordinates $X_m(t)$, associated with complex flutter circular frequency ω, are introduced as follows:

$$X_m(t) = X_{m0} \cdot e^{i\omega t}, X_{m0} = X_{m0}^R + i \cdot X_{m0}^I$$
$$\omega = \omega_R + i \cdot \omega_I = (1 + i \cdot h) \cdot \omega_R \quad (17)$$

$[(X_{m0}^R)^2 + (X_{m0}^I)^2]^{1/2}$: the amplitude of the *m*-th mode ($= |X_{m0}|$)
$\theta_m = tan^{-1}(X_{m0}^I / X_{m0}^R)$: the phase – shift of the *m*-th mode (*rad*) (18)

where ω_R is the flutter circular frequency[rad/s] and $h=\omega_I/\omega_R(=\delta/2\pi)$ is the sum of structural and aerodynamic damping.
The complex eigenvalue equations, derived from inserting $X_m(t)$ of Eq.(17) into Eq.(14) are as follows.

$$([\mathrm{G_{mn}}] - [\lambda]) \cdot \{\mathrm{X_{m0}}\} = \begin{bmatrix} \mathrm{G_{11}} - \lambda & \mathrm{G_{12}} \cdots & \mathrm{G_{1m}} \\ \mathrm{G_{21}} & \mathrm{G_{22}} - \lambda & \mathrm{G_{2m}} \\ \cdot & \cdot & \cdot \\ \cdot & \cdot & \cdot \\ \mathrm{G_{m1}} & \mathrm{G_{m2}} \cdots & \mathrm{G_{mm}} - \lambda \end{bmatrix} \cdot \begin{Bmatrix} \mathrm{X_{10}} \\ \mathrm{X_{20}} \\ \cdot \\ \cdot \\ \mathrm{X_{m0}} \end{Bmatrix} = 0 \quad (19)$$

$$G_{mm} = [F_{mm} + 1 + i \cdot \{E_{mm} - 2h_m^s \cdot (\omega_m/\omega)\}]/\omega_m^2$$
$$G_{mn} = [(F_{mn} + i \cdot E_{mm})/\omega_m^2 (m \neq n)]$$
$$[\lambda] = \mathrm{Diag}[1/\omega^2](\mathrm{Diag.matrix}) \quad (20)$$

For a set of eigen-vectors $\{X_{m0}\}$ to have solution:

$$det([G_{mn}] - [\lambda]) = det[G_{mn}] - Diag\,[1/\omega^2] = 0 \quad (21)$$

Eq.(21) contains the complex unknown ω, then arbitrary initial values (e.g., $\omega_m/\omega=1$) may be given (the choice of ω_m is briefed below) and ω and $\{X_{m0}\}$ can be determined with iterative calculations of Eqs.(20) and (21). The following convergence criterion is appropriate with ε- value of 10^{-3}~10^{-4} (k: number of iterations).

$$|\omega_k - \omega_{k-1}|/|\omega_k| < \varepsilon \quad (22)$$

Once ω is determined, logarithmic damping $\delta = 2\pi \cdot \omega_I/\omega_R$ may be plotted against

wind velocity $V = B \cdot \omega_R / K_0$ for a typical member, where K_0 is an arbitrarily given reduced frequency.

3.3 2-DOF Coupled Flutter

Section model wind tunnel tests consist of only vertical and torsional motions. Therefore the eigen-mode function $\{\varphi_{im}\}$ is reduced to the following form;

$$\{\emptyset_{im}\} = \{0, \emptyset_{im}^{y}, 0, \emptyset_{im}^{\alpha}, 0, 0\} \tag{23}$$

Only $H^*_{ji}(K_i)$ and $A^*_{ji}(K_i)$ were used for 2-DOF flutter analysis. Vibrational data is summarized in Table 4 and flutter velocity is 96.5m/s (Fig. 9). Generally speaking the flutter velocity of 2-DOF is safety side evaluation; because the motions of cables and towers are neglected therefore total damping becomes small.

Table 4 Vibration Characteristics of 2-DOF Model

Notation		Unit	Value
B	Bridge Deck Width	m	60
A	Projection Area per Unit Length	m	4.68
f_h	Natural Frequency of Vertical Motion	Hz	0.0634
f_θ	Natural Frequency of Torsional Motion	Hz	0.0895
m	Mass per Unit length	t/m	60.2
I	Inertia Mass per Unit Length	tm^2/m	32,421
δ_h	Structural Damping of Vertical Motion	-	0.0628 (h = 1%)
δ_θ	Structural Damping of Torsional Motion		

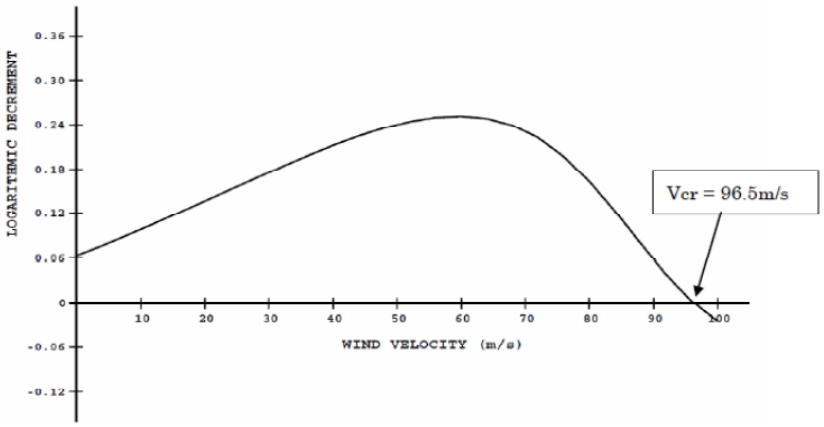

Fig.9 $V-\delta$ Curve of 2D-analysis

3.4 3-Dimensional Flutter Analysis

Input

3-Dimensional multi-flutter analysis was carried out by using input data in Table 5. Two cases were executed as follows.

●Case 1 .....Torsional key mode is asymmetric first

●Case 2 .....Torsional key mode is symmetric first

First twenty modes are used for coupling except for torsional key mode.

Table 5 Outlines of Input Data of 3D Flutter Analysis

<table>
<tr><td>Cross Section</td><td>① Bridge Deck
B = 60m, A = 4.68m
② Cable
D (Outer diameter)= 12m, B = 2.4m (2 times of outer diameter)
③ Tower of Upstream and Downstream side
B = 12m, D = 20m</td></tr>
<tr><td>Static Aerodynamic Force</td><td>① Bridge Deck : Experimental data at α=0deg.
② Cable : C_D = 0.7(by HSB(2002))
③ Hanger Cable : No consideration
④ Tower : C_D = 1.8 (by HSB(2002))</td></tr>
<tr><td>Flutter Derivatives</td><td>① Bridge Deck
<table>
<tr><td colspan="2" rowspan="2"></td><td colspan="6">Motion</td></tr>
<tr><td colspan="2">Sway</td><td colspan="2">Vertical</td><td colspan="2">Rotational</td></tr>
<tr><td colspan="2"></td><td>Vel.</td><td>Disp.</td><td>Vel.</td><td>Disp.</td><td>Vel.</td><td>Disp.</td></tr>
<tr><td rowspan="3">Force</td><td>Drag</td><td>$\mathrm{Q}(P_1^*)$</td><td>-</td><td>$\mathrm{Q}(P_0^*)$</td><td>-</td><td>$\mathrm{Q}(P_3^*)$</td><td>-</td></tr>
<tr><td>Lift</td><td>$\mathrm{Q}(H_0^*)$</td><td>-</td><td>$\mathrm{M}(H_1^*)$</td><td>$\mathrm{M}(H_4^*)$</td><td>$\mathrm{M}(H_2^*)$</td><td>$\mathrm{M}(H_3^*)$</td></tr>
<tr><td>Moment</td><td>$\mathrm{Q}(H_0^*)$</td><td>-</td><td>$\mathrm{M}(A_1^*)$</td><td>$\mathrm{M}(A_4^*)$</td><td>$\mathrm{M}(A_2^*)$</td><td>$\mathrm{M}(A_3^*)$</td></tr>
</table>
Remarks) Q : quasi steady theory,
M : measured data by forced vibration method
② Cable
H_1^* was calculated by quasi steady theory.</td></tr>
<tr><td>Structural Damping</td><td>Lateral : logarithmic decrement δ = 0.0251 (i.e. h = 0.4%)
Vertical and Torsional: logarithmic decrement δ = 0.0628 (h = 1%)</td></tr>
</table>

Air Density	0.12 ($kg \cdot s^2/m^4$)

Output

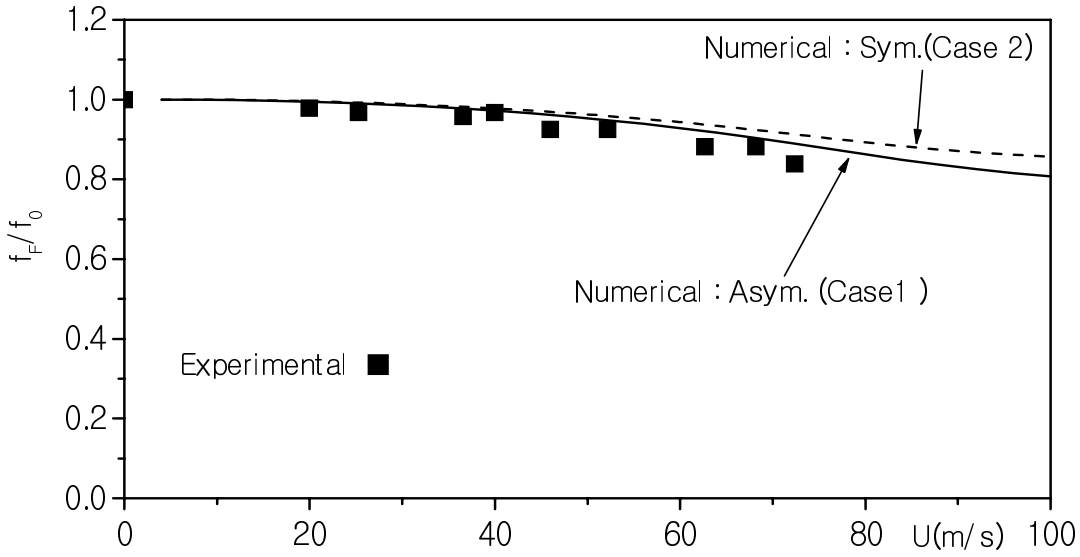

(a) $V-\delta$ Flutter Frequency Curves

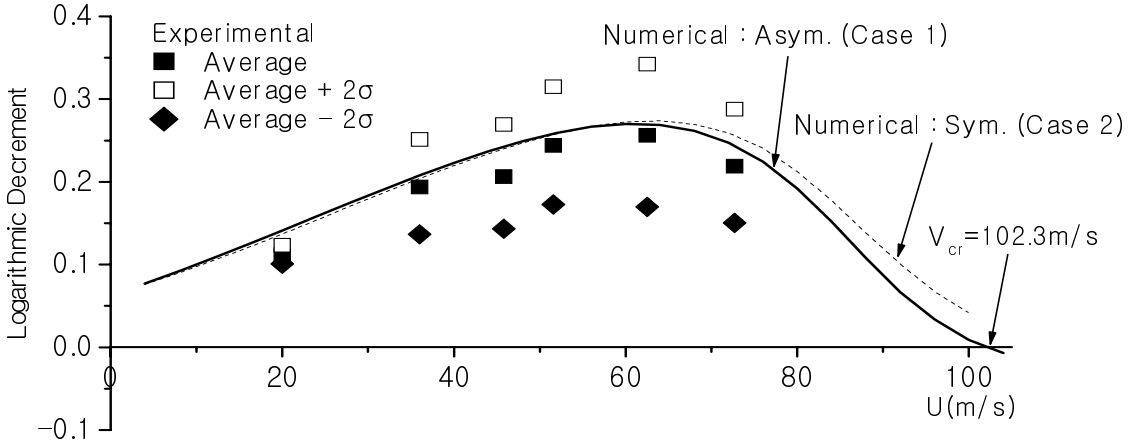

(b) V – δ Curves

Fig.10 Results of 3D Flutter Analysis

Results

Case 1 gives lower flutter velocity therefore key torsion mode is asymmetric. Flutter velocity is almost 100m/s which fulfill the design wind velocity 75m/s. Our method shows good agreement with frequency curve and damping change of

experiments (Fig.10). The flutter mode is asymmetric(Fig.11). As the flutter mode, asymmetric mode is not so many. The side span decks are very short and uncommon then this may happen. The reason might be controversy. As concerning to the estimation of flutter velocity, Samsung is upper bound; DPM is median and YNU is lower bound. This result is mainly due to the difference of asymmetric torsion frequencies (NB: mode No.6 in Table 3).

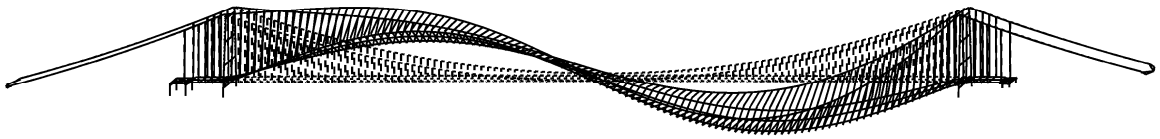

Fig.11 Flutter Mode by Samsung C&T

4. GUST RESPONSE ANALYSIS

4.1 Outline of gust response analysis

Davenport (1962) made a notable first contribution to the buffeting problem. Scanlan (1978) extended it, employing a set of flutter derivatives. Based upon these theories, Tanaka and Yamamura (1988) made the formulation of the gust response for a flexible multi-degree-of-freedom (MDF) system. In this paper, some extensions were achieved to Tanaka and Yamamura (1988) by adding following flutter derivatives terms (e.g., $P_{4i}^*, P_{5i}^*, H_{4i}^*, H_{5i}^*, A_{4i}^*, A_{5i}^*$).

The gust (i.e. buffeting) response equations of motion are derived by inserting Eqs. (9)~(12) into Eq.(4) and modifying the damping ratio and circular frequency:

$$\ddot{X}_m(t) + 2\tilde{h}_m \cdot \tilde{\omega}_m \cdot \dot{X}_m(t) + \tilde{\omega}_m^2 \cdot X_m(t) = \{\emptyset_{im}\}^T \cdot \{F_{im}^B(t)\}/M_m^* \tag{24}$$

$$\left.\begin{aligned} \tilde{\omega}_m &= \omega_m \cdot \left[1 + (\rho/2M_m^*) \cdot \sum_i B_i \cdot \{\phi_{im}^y, \phi_{im}^z, \phi_{im}^\alpha\}^T \cdot [\tilde{\Omega}] \cdot \{\phi_{im}^y, \phi_{im}^z, \phi_{im}^\alpha\} \cdot L_i\right]^{-1/2} \\ \left[\tilde{\Omega}\right] &= \begin{bmatrix} H_{4i}^*(\tilde{K}_i) \cdot B_i & H_{5i}^*(\tilde{K}_i) \cdot B_i & H_{3i}^*(\tilde{K}_i) \cdot B_i^2 \\ P_{4i}^*(\tilde{K}_i) \cdot A_i & P_{5i}^*(\tilde{K}_i) \cdot A_i & P_{3i}^*(\tilde{K}_i) \cdot A_i \cdot B_i \\ A_{4i}^*(\tilde{K}_i) \cdot B_i^2 & A_{5i}^*(\tilde{K}_i) \cdot B_i^2 & A_{3i}^*(\tilde{K}_i) \cdot B_i^3 \end{bmatrix} \end{aligned}\right\} \tag{25}$$

$$\left.\begin{aligned} \tilde{h}_m &= h_m^S \cdot (\omega_m/\tilde{\omega}_m) - (\rho/2M_m^*) \cdot \sum_i B_i \cdot \{\phi_{im}^y, \phi_{im}^z, \phi_{im}^\alpha\}^T \cdot [\tilde{H}] \cdot \{\phi_{im}^y, \phi_{im}^z, \phi_{im}^\alpha\} \cdot L_i \\ \left[\tilde{H}\right] &= \begin{bmatrix} H_{1i}^*(\tilde{K}_i) \cdot B_i & H_{0i}^*(\tilde{K}_i) \cdot B_i & H_{2i}^*(\tilde{K}_i) \cdot B_i^2 \\ P_{0i}^*(\tilde{K}_i) \cdot A_i & P_{1i}^*(\tilde{K}_i) \cdot A_i & P_{2i}^*(\tilde{K}_i) \cdot A_i \cdot B_i \\ A_{1i}^*(\tilde{K}_i) \cdot B_i^2 & A_{0i}^*(\tilde{K}_i) \cdot B_i^2 & A_{2i}^*(\tilde{K}_i) \cdot B_i^3 \end{bmatrix} \end{aligned}\right\} \tag{26}$$

where $\tilde{\omega}_m$ and $\tilde{h}_m$ are, respectively, the equivalent circular frequency

and equivalent damping ratio in the wind. $\{F_{im}^{B}(t)\}$ is the buffeting force of the *m*-th mode. Eq.(25) is implicit function of $\tilde{\omega}_m$, therefore, an iterative calculation is necessary to obtain $\tilde{\omega}_m$.

A structure becomes unstable if the equivalent damping ratio $\tilde{h}_m$ (Eqs.(26)) becomes negative. The equations above apply to the stiffening girder. For other members, simplification is possible. For example, only P_{1i}^{*} and H_{1i}^{*} are necessary for cables and only P_{1i}^{*} for tower members.

In addition, the special correlations function (i.e., coherence) by Davenport (1962): $Coh(f) = exp\left[-kf\Delta Y / U\right]$ is modified to the following expression (Hatanaka (1995));

$$Coh(f) = exp\left[-k(f + f_0)\Delta Y / U\right] \tag{27}$$

Where *k* is decay factor, *f* is frequency and f_0 is frequency-shift parameter to fit experimental data as shown Fig.12. The number of f_0=0.22 and f_0=0.44 are applied respectively for horizontal and vertical wind gust components. The purpose of modification is to avoid overestimation of gust response which we will refer later.

Space limitations prohibit a detailed presentation of our gust response method. Frame work of the method is almost same as the reference (Tanaka 1988).

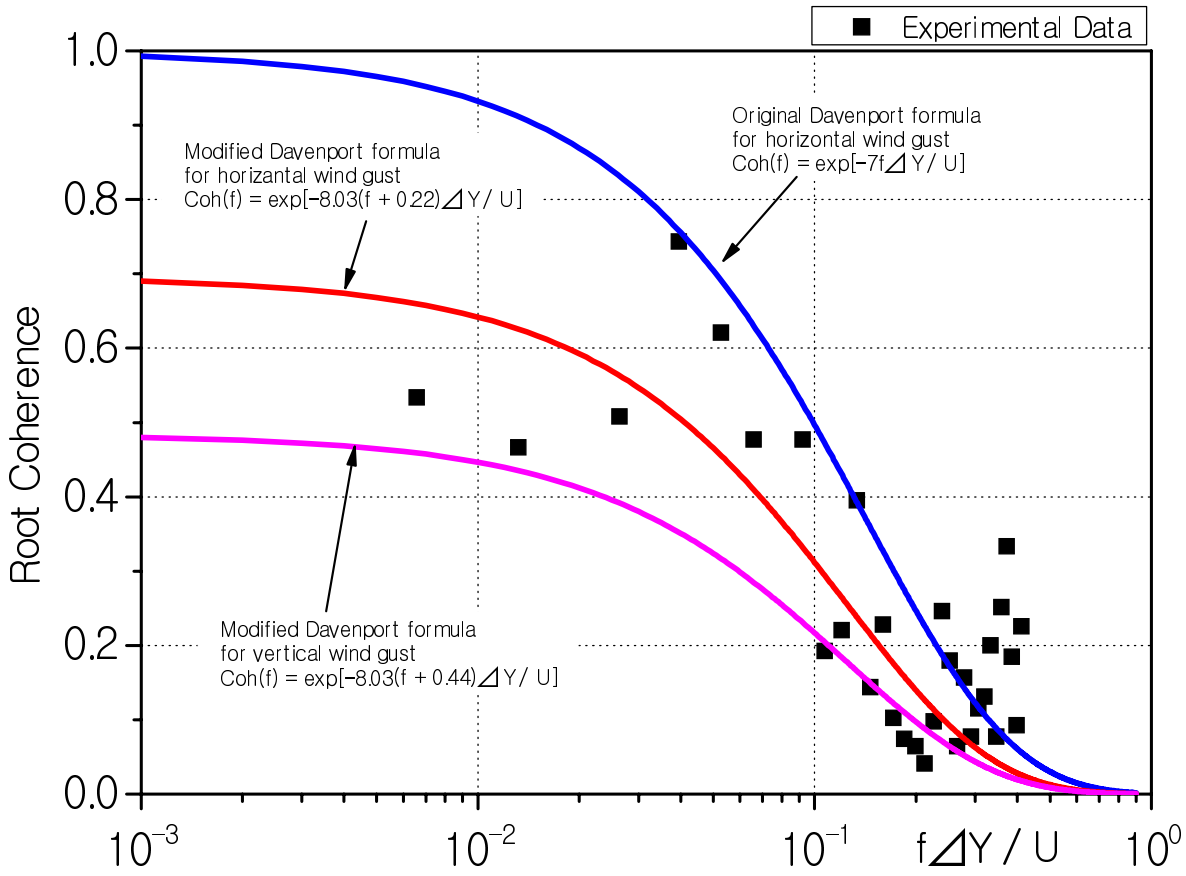

Fig.12 Span-Wise Coherence of Horizontal Wind Gust
(Original and Modified Davenport formula, ⊿Y=12.5m)

4.2 Application to the Messina Bridge

Input data

- Power Spectral Density (PSD)
  Fitting curves were used instead of the measured PSD in boundary layer turbulent flow shown In Fig. 13 (Red curves).
- Static aerodynamic coefficients (Fig.5 and Table 2 and 5)
- Flutter derivatives (Figs.6 and 7) and Eq. (7)
- Aerodynamic admittance: Drag; Davenport Formula,
  Lift and Moment; Experimental data (Fig. 14)
- Power law of vertical wind profile $\alpha = 0.11$ and wind velocity is 60m/s at the bridge deck height of the mid span
- Maximum peak factor: Davenport (1964) (T= 600 sec)
- Structural damping (Table 5)
- Number of summed modes: 50

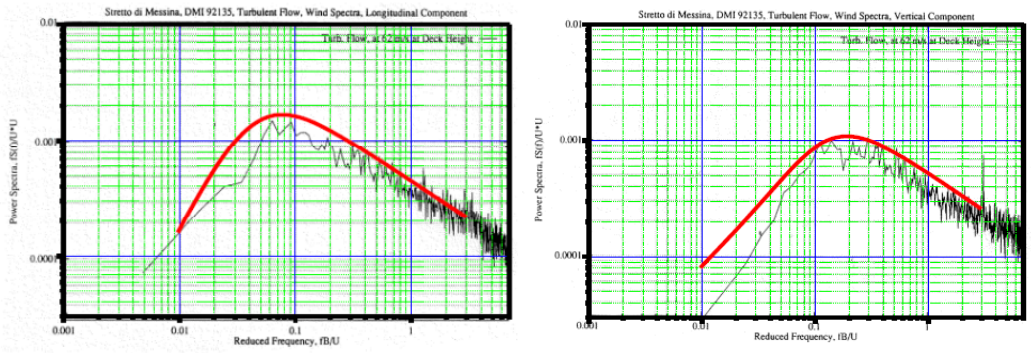

(a) Horizontal Component (b) Vertical Component

Fig. 13 Power Spectrum Density given by PDM

Results of our gust response analysis are compared with those of PDM and wind tunnel experimental data by DMI (Diana 1999) in Table 6.

First we tried the gust response analysis applying Davenport' coherence and compared the results with those of PDM and experiment. Then we found our results are almost same as those of PDM as you see in Table 5 (e.g., discrepancy: 12~16% on RMS). However the RMS of lateral displacement shows very large error (i.e. 6.46).

This tendency was already known by the analyses of the AKASHI KAIKYO Bridge and the KURUSHIMA 2nd Bridge (Toriumi (1997)). To overcome the discrepancy, modified Davenport formula (i.e. Eq. (27)) was derived by Hatanaka (1995). By the use of Eq. (24), the discrepancy became much smaller as shown in Table 6. We must be very careful to apply Davenport's coherence for applying long span bridges. Davenport formula discards the effect of turbulence scale. When bridge span (e.g., typically more than about 1000m) becomes long and the bridge's national frequencies become small, his coherence will become overestimation (Irwin H.P.A.H 1977).

Fig.14 shows the experimental admittance (symbol:■) and Sears' functions of lift and moment forces. The discrepancy around main modes is large. Then we used the experimental values. Satisfactory results are obtained as shown in Table 6.

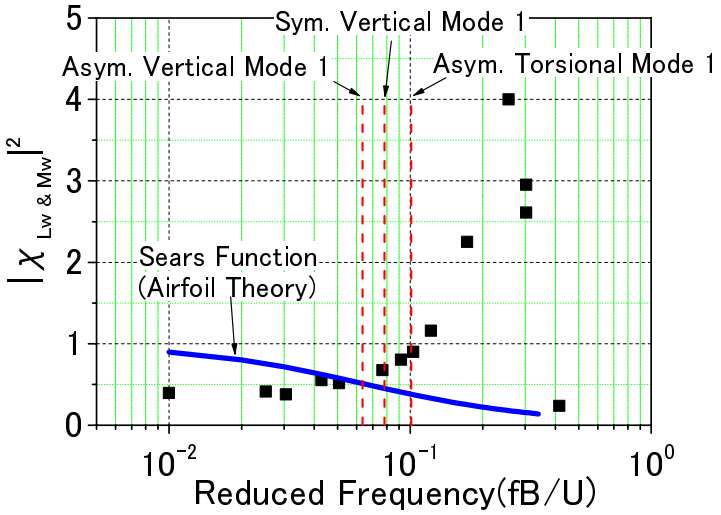

Fig. 14 Comparison between Sears Function and Experiments

Table 6 Results of Gust Response Analysis

		Gust Response Analysis		Experiment	Error	
		SAMSUNG(①)	PDM(②)	(③)	①/②	①/③
Lateral at mid span (m)	Mean	9.91	9.49	8.36	1.04	1.19
	RMS	0.55 (1.81)	–	0.28	–	1.96(6.46)
	Max	11.42 (14.78)	–	–	–	–
Vertical at mid span (m)	Mean	-0.38	–	–	–	–
	RMS	0.20 (0.44)	–	0.26	–	0.77(0.59)
	Max	-1.01(-1.69)	–	–	–	–
Vertical at quarter span(m)	Mean	-0.30	–	–	–	–
	RMS	0.21 (0.50)	0.43	0.29	0.49(1.16)	1.39(1.51)
	Max	-0.94 (-1.79)	–	–	–	–
Rotational at mid span (deg.)	Mean	0.64	0.52	0.40	0.81	1.60
	RMS	0.19 (0.29)	0.26	0.17	1.37(1.12)	1.12(1.71)
	Max	1.24 (1.53)	–	–	–	–

NB. The values in () are the results by Davenport's coherence

5. CONCLUSION

This paper describes flutter and gust response analyses using 3D frame model of the Messina Strait Bridge for the benchmark study. The results of the paper are summarized as follows:

(1) Eigen Mode Analysis

The eigen-frequency by our analysis agreed to the original results by PDM within about 10% error. It is interesting that the lowest frequency modes of vertical and torsional motions are both asymmetric.

(2) Flutter Analysis

The flutter onset velocity of 2D and 3D frame model are respectively 95.1 and 102.3 m/s. The analysis results on flutter frequency and logarithmic damping agree well to the experimental results. The flutter mode was asymmetrical mode shape.

(3) Gust Response Analysis

To improve gust response analysis, Davenport formula was modified to fit the experimental data of the spatial correlation. Also, the experimental data of the aerodynamic admittance functions for lift and moment forces were used instead of Sears' function. By these methods, the RMS of our analysis and experimental result became satisfactory close. However our approximation of PSD is somewhat larger in low frequency range. Best fitting method of PSD may be future challenge.

We hope that this paper will contribute to the bench making assessment for the Messina Bridge.

Finally we express sincere appreciations to YNU for the receipt of the 3D-frame model data.

REFERRENCES

Davenport A.G. (1962),"Buffeting of a Suspension Bridge by Storm Winds", *J. of Structure Div., ASCE*, Vol.88 No.ST3, 233-268

Davenport A.G. (1964), "Note on the Distribution of the Largest Value of a Random Function with Application to Gust Loading", *Proc.. ICE*, 187-196

Diana, G., Falco, M., Cheli, F. and Cigada, A (1999), "Experience Gained in the Messina Bridge Aeroelastic Project", *Long-Span Bridges and Aerodynamics,* Springer Verlag, Tokyo

Diana, G., Zasso, A. and Rocchi, D. (2001), "Benchmark study on wind bridge response", *J. of Wind Engineering*, No. 89, 393-396.

Hatanaka A., Ogasawara M., Katsuchi H. and Yamamura N. (1995),"Coherence for Buffeting Response Analysis of Long-Span Bridges", *J. of Steel Construction*,

Vol.3, November (in Japanese)
Honshu-Shikoku Bridge Authority (HSB) (2002),"*Wind Resistant Design Code of the Honshu-Shikoku Bridge"* (in Japanese)
Irwin H.P.A.H.(1977), "Wind Tunnel and Analytical Investigations of the Response of Lions' Gate Bridge to a Turbulent Wind", *National Research Council Canada*,10-12
Scanlan R.H (1978), "The Action of Flexible Bridges under Wind, Part 1(Flutter Theory)", *J. of Sound and Vibration*, 60-2, 187-199
Scanlan R.H (1978),"The Action of Flexible Bridges under Wind, Part 1(Buffeting Theory)", *J. of Sound and Vibration*, 60-2, 201-211
Simiu E. and Scanlan R.H. (1996), "*Wind Effects on Structures"*, Interscience publication
Stretto di Messina S.p.A (2009), *"The Messina Strait Bridge - A challenge and a dream –"*, CRC Press
Tanaka H., Yamamura N. and Shiraishi N. (1993), "Multi-Mode Flutter Analysis and Two & Three Dimensional Model Tests on Bridges with Non-Analogous Modal Shapes", *Structural Eng/Earthquake Eng. Vol.10, No.2*, 71-81
Tanaka H., Yamamura N. and Tatsumi M. (1988), "The 3-Dimensional Buffeting Response Analysis of Flexible MDF Systems", *International Colloquium on Bluff Body Aerodynamics, J. of Wind Engineering No.37*, 665-674
Toriumi R., Yamamura N. and Tanaka H. (1997), "Study on Buffeting Response Analysis of Long Span Bridges", *J. of Steel Construction*, Vol.4, No.13, 45-52
(in Japanese)
Yamada ,H., and Katsuchi, H. (2003), "Comparative analysis of Messina Bridge - International benchmark study", *Eleventh International Conference on Wind Engineering, Lubbock, Texas, USA*, 131-138